



This discussion paper is/has been under review for the journal Atmospheric Chemistry and Physics (ACP). Please refer to the corresponding final paper in ACP if available.

# Meteorological factors controlling low-level continental pollutant outflow across a coast

D. L. Peake, H. F. Dacre, J. Methven, and O. Coceal

Department of Meteorology, University of Reading, Earley Gate, Reading, Berkshire, RG6 6BB, UK

Received: 11 March 2014 – Accepted: 27 March 2014 – Published: 30 April 2014

Correspondence to: H. F. Dacre (h.f.dacre@rdg.ac.uk)

Published by Copernicus Publications on behalf of the European Geosciences Union.

## Coastal outflow

D. L. Peake et al.

Title Page

Abstract

Introduction

Conclusions

References

Tables

Figures



Back

Close

Full Screen / Esc

Printer-friendly Version

Interactive Discussion



## Abstract

Coastal outflow describes the horizontal advection of pollutants from the continental boundary layer across a coastline into a layer above the marine boundary layer. This process can ventilate polluted continental boundary layers and thus regulate air quality in highly populated coastal regions. This paper investigates the factors controlling coastal outflow and quantifies its importance as a ventilation mechanism. Tracers in the Met Office Unified Model (MetUM) are used to examine the magnitude and variability of coastal outflow over the eastern United States for a 4 week period during summer 2004. Over the 4 week period, ventilation of tracer from the continental boundary layer via coastal outflow occurs with the same magnitude as vertical ventilation via convection and advection. The relative importance of tracer decay rate, cross-coastal advection rate, and a parameter based on the relative continental and marine boundary layer heights, on coastal outflow is assessed by reducing the problem to a time-dependent box-model. The ratio of the advection rate and decay rate is a dimensionless parameter which determines whether tracers are long-lived or short-lived. Long- and short-lived tracers exhibit different behaviours with respect to coastal outflow. For short-lived tracers, increasing the advection rate increases the diurnally averaged magnitude of coastal outflow, but has the opposite effect for very long-lived tracers. Short-lived tracers exhibit large diurnal variability in coastal outflow but long-lived tracers do not. By combining the MetUM and box-model simulations a landwidth is determined which represents the distance inland over which emissions contribute significantly to coastal outflow. A landwidth of between 100 and 400 km is found to be representative for a tracer with a lifetime of 24 h.

## 1 Introduction

Coastal outflow is defined as the horizontal advection of pollutants across a coastline at a height above the marine boundary layer ( $H_{\text{MBL}}$ ) and below the maximum height that

ACPD

14, 10853–10890, 2014

## Coastal outflow

D. L. Peake et al.

Title Page

Abstract

Introduction

Conclusions

References

Tables

Figures

⏪

⏩

◀

▶

Back

Close

Full Screen / Esc

Printer-friendly Version

Interactive Discussion



## Coastal outflow

D. L. Peake et al.

[Title Page](#)[Abstract](#)[Introduction](#)[Conclusions](#)[References](#)[Tables](#)[Figures](#)[Back](#)[Close](#)[Full Screen / Esc](#)[Printer-friendly Version](#)[Interactive Discussion](#)

the continental boundary layer reaches during its diurnal cycle ( $H_{\max}$ ) (Dacre et al., 2007). Pollutants emitted over land can be mixed to the top of the continental boundary layer during the day through vertical turbulent mixing by boundary layer scale eddies and can then be exported horizontally above  $H_{\text{MBL}}$ . Pollutants with a long enough life-time can continue to undergo coastal outflow during the nighttime due to their remaining presence in the residual layer which is left behind as the continental boundary layer height collapses at nightfall.

Coastal outflow is a potentially important mechanism for the ventilation of continental boundary layers and regulation of air quality in coastal regions. Human population tends to be concentrated in coastal regions and consequently so are pollutant sources from industrial and residential areas, as well as road traffic and other transportation. Episodes of poor regional air quality often occur in anticyclonic situations where the large-scale flow is relatively stagnant, reducing outflow, and vertical ventilation of the boundary layer is also inhibited, for example by descending dry air creating a strong inversion at the boundary layer top. In this article, a month-long mesoscale model simulation of summer 2004 over the eastern side of North America is used to investigate the relative importance of coastal outflow and vertical ventilation for pollutant levels within the continental boundary layer. In addition, the evolution of the tracer distribution is summarised in terms of a box model with only a few parameters controlling the behaviour. The box model is sufficiently simple to have analytic solutions, but is also capable of describing the diurnal and synoptic timescale variability in tracers in the mesoscale model.

The month chosen for investigation was during the intensive observing period of the ICARTT (International Consortium for Atmospheric Research on Transport and Transformation) experiment in summer 2004 (Fehsenfeld et al., 2006). ICARTT was an umbrella organisation for more than 100 collaborations that focused on transport and chemical transformation across the eastern USA and then spanning the North Atlantic to Europe. The observations of most relevance for this study were associated with the ground-based network enhanced as part of the New England Air Quality Study

## Coastal outflow

D. L. Peake et al.

[Title Page](#)[Abstract](#)[Introduction](#)[Conclusions](#)[References](#)[Tables](#)[Figures](#)[Back](#)[Close](#)[Full Screen / Esc](#)[Printer-friendly Version](#)[Interactive Discussion](#)

(NEAQS), including more than 100 ground sites measuring chemical constituents and 7 boundary layer wind profilers measuring continuously throughout the period (5 min resolution). There were no prolonged periods of flow stagnation during this summer, and therefore there were no episodes of particularly poor regional air quality. However, there were marked episodes of cross-coastal pollutant transport, some of which was observed by research aircraft as the air crossed the Atlantic to the Azores and Europe (Methven et al., 2006; Owen et al., 2006).

Stratified layers of pollutants over oceans have been observed by many studies (Paluch et al., 1992; Müller et al., 2001; Davis et al., 2012). Pollutants exported above  $H_{\text{MBL}}$  have longer lifetimes (Dickerson et al., 1999), are decoupled from the surface by the inversion at the top of the MBL (Vickers et al., 2001), and are subject to less dry deposition, lower humidity and higher wind speeds than tracer exported below  $H_{\text{MBL}}$  (Skylingstad et al., 2005), allowing more efficient long-range transport of pollutants (VanCuren et al., 2005; Holzer and Hall, 2007). These are often observed as distinct layers of pollution at altitudes between 500 m and 3 km (Verma et al., 2006).

Angevine et al. (2006) observed the formation of stable marine boundary layers over the cool waters of the Gulf of Maine in the summer of 2004. A sharp cooling of 5 to 15 K occurred in the lowest (approximately) 100 m of air within 30 min of the air crossing the coast. Turbulence was greatly reduced in this layer of the atmosphere. Skylingstad et al. (2005) performed a large eddy simulation and showed that turbulence was damped from the surface upwards whilst a maximum in turbulence remained at the top of the MBL for 20 km offshore. The decoupling from the surface occurred very quickly after air flowed over the cool sea, allowing pollutants exported by coastal outflow to become isolated from the surface flow.

Whilst studies have observed (Müller et al., 2001) and modeled (Davis et al., 2012) individual coastal outflow events, this paper presents a study which analyses coastal outflow over a 4 week period. Simulations using an operational numerical weather prediction model and a simple box model are performed to determine the meteorological variables controlling coastal outflow. A box-model with simplified meteorology is used

## Coastal outflow

D. L. Peake et al.

[Title Page](#)[Abstract](#)[Introduction](#)[Conclusions](#)[References](#)[Tables](#)[Figures](#)[⏪](#)[⏩](#)[◀](#)[▶](#)[Back](#)[Close](#)[Full Screen / Esc](#)[Printer-friendly Version](#)[Interactive Discussion](#)

to investigate the relative importance of three variables; tracer lifetime, cross-coastal wind speed and ratio of  $H_{\max}$  to  $H_{\text{MBL}}$  in controlling coastal outflow. Results of the two models are then compared to estimate the width of land over which emissions contribute significantly to coastal outflow.

5 The Met Office Unified Model (MetUM) and experimental design are described in Sect. 2 and the simulated winds are evaluated using wind profiler observations throughout the period. The variability in tracer burden across the land within the domain is compared with the regional pollution estimated from a network of ground-based stations measuring carbon monoxide. The structure of the box-model is introduced in Sect. 3  
10 and used to quantify the relative magnitudes of ventilation from the boundary layer over the eastern USA by coastal outflow and vertical transport. Evolution equations for the box model are derived in Sect. 4 and used to map out the behavior of tracer in parameter space. The magnitude and diurnal variability of coastal outflow in the mesoscale simulation are interpreted using the box model in Sect. 5 which allows an understanding  
15 of the parameters that have most influence on coastal outflow amounts.

## 2 Four-week mesoscale model simulation

### 2.1 Model and experiment specification

The Met Office Unified Model (MetUM) is used to simulate the atmosphere over a domain containing the eastern half of the United States and western half of the Atlantic Ocean (Fig. 1). The 27 day period 00:00 UTC, 13 July 2004 to 23:00 UTC, 8 August  
20 2004 was chosen to coincide with the ICARTT field campaign measurements. The MetUM version 6.1 is run with 5 min timesteps and a horizontal gridspacing of  $0.11^\circ$  ( $\sim 12$  km) in both the longitude (250 gridpoints, a western boundary of  $85.92^\circ$  W) and latitude (271 gridpoints, a southern boundary of  $23.77^\circ$  N) directions. The simulation  
25 uses the v6.1 level configuration that was used for operational numerical weather prediction: 38 terrain-following model levels in the vertical, with 10 levels in the lowest

## Coastal outflow

D. L. Peake et al.

[Title Page](#)[Abstract](#)[Introduction](#)[Conclusions](#)[References](#)[Tables](#)[Figures](#)[Back](#)[Close](#)[Full Screen / Esc](#)[Printer-friendly Version](#)[Interactive Discussion](#)

2 kma.g.l., and model top at 39 km. The simulation is initialised at 0000Z 13 July 2004 by re-gridding a global operational re-analysis from the European Centre for Medium-Range Weather Forecast (ECMWF) archive with a gridspacing of  $0.25^\circ \times 0.25^\circ$  lat/lon, (approximately  $22\text{ km} \times 27\text{ km}$ ). Free-running global MetUM forecasts (approximately  $30\text{ km} \times 65\text{ km}$  gridspacing) from each six-hourly ECMWF operational re-analysis (available at 00Z, 06Z, 12Z and 18Z) provide hourly updates for the lateral boundary conditions used in the MetUM simulation. Sea surface temperatures are set to climatology.

An important aspect for this study is the diagnosis of boundary layer depth from the model. At each horizontal gridpoint, the boundary layer is defined by the number of turbulent mixing levels (NTML). For stable conditions this is the region in contact with the surface where the bulk Richardson number is smaller than 1. For unstable conditions an adiabatic moist parcel ascent is performed in the model; ascent is stopped when the parcel becomes negatively buoyant. If the layer is well mixed the NTML is set to the parcel ascent top (inversion height). If the layer is cumulus capped the NTML is set to the lifting condensation level (cloud base) (Lock et al., 2000). The residual layer is defined to extend from the top of the boundary layer to  $H_{\text{max}}$ , a height representing the deepest extent of the continental boundary layer across the region throughout all days. In practice, the maximum boundary layer height was found every day at each land point, and  $H_{\text{max}}$  was defined by the 90th percentile using all data from the 27 day model run. It was found to be 2000 m and to vary little from day to day. The free tropospheric layer represents a layer extending from the top of the residual layer to the top of the atmosphere in the simulation.

Coastal outflow in the model will depend on the representation of horizontal flow across the coast. The quality of cross-coastal winds in the 27 day simulation is illustrated using observations taken with a 915 MHz Doppler radar wind profiler sited at Pease, New Hampshire, which was at the focus of activity for the ICARTT experiment (Fehsenfeld et al., 2006). The profiler is part of the NOAA-DOE Cooperative Agency Radar Wind Profiler Network. The data has a vertical resolution of 60 m (Carter et al., 1995). At this location, the terrain is flat (site at 30 m a.s.l.) and the coast is oriented in

## Coastal outflow

D. L. Peake et al.

[Title Page](#)[Abstract](#)[Introduction](#)[Conclusions](#)[References](#)[Tables](#)[Figures](#)[Back](#)[Close](#)[Full Screen / Esc](#)[Printer-friendly Version](#)[Interactive Discussion](#)

approximately the same direction as the average for the East Coast USA (see Fig. 1). Figure 2 shows the component of the horizontal wind perpendicular to the coast vs. height on a time series obtained from the MetUM and wind profiler. In both cases, the diurnal cycle has been filtered from the data using a running mean with a centred 24 h window. The synoptic variations are clearly represented in the model, indicating that the continuous update of its boundary conditions using analyses is sufficient to keep the synoptic scale evolution on track. There are events with larger differences. For example, the model simulates stronger offshore winds (by as much as  $5 \text{ ms}^{-1}$ ) near the surface from 4 to 5 August 2004. Away from the surface, for example at 2 km, the correspondence is better. Over the whole time series, the standard deviation of the difference between the MetUM wind and profiler is less than  $1 \text{ ms}^{-1}$  at all heights. On average the wind speed in the MetUM is too low at the surface by  $1 \text{ ms}^{-1}$  and too strong at 800 m by  $0.8 \text{ ms}^{-1}$ , without significant bias above 1500 m. The height dependence of the bias is in part associated with a weaker sea breeze circulation in the model. Comparing the model with the profiler at Pittsburgh, almost 500 km inland, shows a similar standard deviation, but much smaller bias.

A diurnal composite was constructed for both datasets by removing the 24 h filtered data from the full winds and then compositing the remainder by averaging each hour of the day over the 27 days available. Figure 3 presents the comparison between the MetUM and wind profiler. The observations pick out a marked diurnal cycle in winds. Below 500 m the flow is offshore from 00:00 to 10:00 LT and then onshore from 11:00 to 23:00 LT, as expected for a seabreeze circulation. The average amplitude of onshore or offshore surface winds is  $2 \text{ ms}^{-1}$ . Above 500 m, but below the top of the residual layer at 2000 m, the offshore winds peak 2–4 h after the maximum in the onshore sea breeze, indicative of a return circulation. The model captures some aspects of the sea breeze circulation. The nocturnal land breeze peaks too early in the night and appears to be too shallow and too weak at later times. The subsequent onshore flow at 1000 m is too strong. The evening sea breeze is better represented. Since both the synoptic

and diurnal variability are represented in the simulation, it is reasonable to suppose that the variability in tracer transport can also be simulated realistically.

## 2.2 Tracers in the model

Pollution is represented within the MetUM simulation using two passive tracers, both with e-folding lifetimes of 24 h, initialised and continuously emitted in the lowest model level uniformly over the land (as determined by the land-sea mask of the model). One tracer is transported by advection, parameterised convective mass fluxes and turbulent mixing, and the other is transported by advection and turbulent mixing only. Whilst the effects of the different transport processes on tracer distribution are not simply additive, by preventing one of the tracers being transported via convection the relative importance of convection to be quantified. Figure 1 illustrates the tracer distribution during the major coastal outflow event of the ICARTT campaign period.

The total mass of tracer in the domain takes four days to reach a quasi-steady state, where the emission rate balances the tracer decay rate, and is approximately equal to  $S\alpha$ , where  $S$  is the total source rate in  $\text{kg s}^{-1}$  and  $\alpha$  is the tracer lifetime. The uniform surface emission rate is  $10^{-7} \text{ kg m}^{-2} \text{ s}^{-1}$  and the land area  $3.91 \times 10^{12} \text{ m}^2$ . The emission rate was chosen to spin-up to an average steady state mixing ratio across the whole domain of the order of 500 ppbv (assuming tracer is spread uniformly across the whole domain in a layer of depth 1 km and land occupies half the domain).

The tracer experiment is idealised, assuming uniform emission rate across the entire land surface and a uniform decay rate (without chemical reaction). It is hard to evaluate the simulation against data since pollutants have spatial and temporal variability in emissions. However, it would be desirable to know to what extent the idealised tracer yields information relevant to regional air quality. During the period, the Northeast Air Quality Study was taking additional ground-based measurements as a contribution to the umbrella ICARTT experiment. The constituents most widely measured at sites spanning the eastern seaboard of the USA were ozone and carbon monoxide (CO). Since ozone is a secondary pollutant that is produced chiefly through photochemistry

Title Page

Abstract

Introduction

Conclusions

References

Tables

Figures



Back

Close

Full Screen / Esc

Printer-friendly Version

Interactive Discussion



## Coastal outflow

D. L. Peake et al.

[Title Page](#)[Abstract](#)[Introduction](#)[Conclusions](#)[References](#)[Tables](#)[Figures](#)[⏪](#)[⏩](#)[◀](#)[▶](#)[Back](#)[Close](#)[Full Screen / Esc](#)[Printer-friendly Version](#)[Interactive Discussion](#)

rather than surface emission, and has a strong diurnal cycle related to photochemistry, it was not suitable for comparing with the idealised tracer. However, CO has a long photochemical loss timescale (25 days) and is emitted directly by vehicles and industry. Therefore, CO behaves as a passive tracer subject to emissions, advection and mixing.

The emission rates vary greatly across the region, and the sites were closer together in the urban areas near the coast. However, here the focus is on the time series of the regional-average mixing ratio.

The solid line in Fig. 4 presents the time series obtained by averaging over 121 surface sites from the Environmental Protection Agency. The grey shading indicates the range given by plus and minus one standard deviation from the mean. The dashed line is the average tracer mixing ratio within the continental boundary layer (box-1) of the MetUM simulation (south of 44° N since this is the northern extent of the surface sites). Although the variability in CO is large compared with the mean, the domain-mean time series have a positive correlation (0.36). Note that the weekend days have been removed from both time series in this comparison and the remaining week days concatenated together. This is necessary due to the strong drop in CO emissions at the weekend which would not be represented in the idealised tracer. A 24 h running median filter has also been applied to remove the diurnal cycle. Note that the mixing ratios from the model were not re-scaled, but the close match in values is fortuitous, although the emission rate was chosen to give a similar magnitude for the idealised tracer mixing ratios. An appropriate timescale for the decay of anomalies in CO is dominated by mixing with cleaner air and in the range 5–10 days outside the boundary layer. The idealised tracer has a much shorter lifetime (1 day) and so would be expected to spin-up to a quasi-steady state with lower mixing ratios than CO if the same source rate had been prescribed. Nevertheless, the co-variability indicates that the ventilation of tracer out of the continental boundary layer in the model, both by coastal outflow and vertical transport, has an effect on the regional tracer burden that resembles the variability in observed pollution loading across the region.

### 3 MetUM tracer budget partitioned into box-model structure

The evolution of tracer mass within in the MetUM simulation is analysed by partitioning the domain into areas over land and sea and then also in the vertical depending upon boundary layer depth (Fig. 5). The complexity of the situation simulated by the MetUM is reduced to a few variables that describe tracer amounts in these six “boxes” and the fluxes between them. In Sect. 4.1, equations will be derived for a box-model that describes the evolution of the masses in each box and their dependence on a few parameters defining the problem. The Appendix gives an analytical solution to the box model in the simplest situation where the model parameters are constants. The box model represents a way of rationalising the behaviour of regional pollution concentrations and coastal outflow in a realistic model, and the fundamental parameters upon which they depend.

The box model consists of three layers: the boundary layer (box-1 and box-2), the residual layer (box-3 and box-4) and the free tropospheric layer (box-5 and box-6). One column of boxes is above the land (box-1, box-3 and box-5), the other column is above the sea (box-2, box-4 and box-6), and the interface between the two columns lies along the coastline.

The mass of tracer in each box,  $M$ , is calculated for each timestep. The quasi-steady state mass of tracer in each box is represented by numbers in the centre of each box in Fig. 6. It is defined by calculating the percentage of the total domain tracer in that box at each timestep, and then averaging those values over the 27 day period. The arrows indicate the direction of net transport between each box that would be necessary to maintain steady state, given that all the tracer enters the domain at the land surface, but tracer is lost everywhere at the uniform decay timescale of 24 h. The continental boundary layer and continental residual layers are combined (box-1 and box-3) to avoid depicting the large diurnal cycle mass transport between them. The boxes over the sea are assumed to extend sufficiently far downwind from the coast that any tracer entering these boxes decays before it can leave (i.e., no outflow). By construction, the mass

Title Page

Abstract

Introduction

Conclusions

References

Tables

Figures



Back

Close

Full Screen / Esc

Printer-friendly Version

Interactive Discussion



## Coastal outflow

D. L. Peake et al.

Title Page

Abstract

Introduction

Conclusions

References

Tables

Figures

◀

▶

◀

▶

Back

Close

Full Screen / Esc

Printer-friendly Version

Interactive Discussion



transports are defined such that the steady-state mass of each box is decomposed into a sum of transports in, minus the sum of transports out. Differences in the time elapsed along transport pathways is not accounted for in this simple partition, although this would have an influence due to the tracer decay. Therefore, it should be interpreted as depicting the various branching ratios into and out of different boxes. The masses and transports are expressed as a percentage of total tracer in the domain.

To estimate the average transport pathways the following steps are performed. Firstly, the vertical transport of tracer by convection is calculated using the difference in the steady-state masses in the free tropospheric boxes ( $M_5$  and  $M_6$ ) for two tracers: the tracer transported by all processes in the model, minus the tracer that is excluded the convective mass transport scheme. 3.0 units are transported into box-5 via convection over land, while 0.5 units are transported into box-6 via convection over the sea. Tracer transported by convection is assumed not to entrain or detrain tracer into the marine residual layer (box-4).

There remain 6 unknown transports (the black bands in Fig. 6) to obtain from the mass budgets of 5 boxes. For example,  $M_5 = F_{L5} + C_L - F_{56}$  where  $C_L$  is the convective mass transport from the continental BL to box-5 as estimated from step-1,  $F_{L5}$  is the non-convective transport from the CBL to box-5 and  $F_{56}$  is the net horizontal transport from box-5 to box-6. Since one of the five budget equations is not independent, due to the constraint that the box masses sum to 100 %, two further relations are required to solve the simultaneous equations for the six transports:

1. As there is little vertical transport over the sea, all tracer will decay in the same box to which it is advected horizontally. Since the tracer decay rate is the same everywhere, we can assume that the ratio of the horizontal transports from land box (box- $L$ ) into the coastal outflow layer (box-4) and marine boundary layer (box-2),  $F_{L4}/F_{L2}$ , is approximately equal to the ratio of the masses of tracer in box-4 and box-2,  $M_4/M_2 = 3.33$ .

## Coastal outflow

D. L. Peake et al.

Title Page

Abstract

Introduction

Conclusions

References

Tables

Figures



Back

Close

Full Screen / Esc

Printer-friendly Version

Interactive Discussion



2. Assume that the horizontal transport in the free troposphere from box-5 to box-6 is related to the horizontal transport below by a known ratio,  $R = F_{56}/(F_{L2} + F_{L4})$ . One simple assumption based on the mass of tracer available to advect horizontally is that  $R = M_5/M_L$ .

5 These two assumptions were used to solve for the mass transport estimates in Fig. 6. The magnitude of tracer ventilated from the continental boundary layer via coastal outflow is similar to the magnitude of tracer ventilated by vertical processes out of the continental BL (12.4 units by resolved vertical advection and mixing, 3.0 by convective mass fluxes) for the eastern half of the United States (the domain area of the Me-

10 tUM simulation). The horizontal transport from land over the Atlantic is dominated by the coastal outflow layer above the marine boundary layer. In reality, soluble pollutants would also be rapidly deposited to the ocean surface from the marine boundary layer, while they would be somewhat isolated from deposition in the coastal outflow layer above.

## 15 4 Characterising the problem using a time-dependent box-model

### 4.1 Box-model evolution equations

A box-model is now developed to describe the evolution of tracer amounts in the layers above the land and sea introduced in the last section. The aim is to reduce the complexity of the air pollution problem to a simple system described by a few fundamental parameters that can be estimated from data. The behaviour of the reduced system is explored and related to the mesoscale model and atmospheric composition observations.

As with the mesoscale model simulation, pollution is modeled within the box-model using a passive tracer with e-folding lifetime  $\alpha$ . Tracer is emitted at a constant rate in

25 the lowest box over land only (box-1) as a representation of anthropogenic emissions.

Tracer mixing ratio and air density are assumed to be well mixed within each box at any instant.

The horizontal wind,  $U$ , advecting tracer from land to sea is assumed to be eastwards ( $U > 0$ ) and uniform in height and time. There is no vertical advection between boxes. However, transport between the boundary layer and residual layer occurs via entrainment and detrainment as the boundary layer top over land moves up and down with the diurnal cycle.

The boxes over the sea are assumed to extend sufficiently far downwind from the coast that any tracer entering these boxes decays before it can leave (i.e., no outflow). The width of the land boxes ( $L$ ) is an important parameter of the model. This is because the horizontal inflow into the continental boxes from the west is assumed to carry no tracer and therefore  $L$  determines the width of the domain experiencing emissions and therefore the total tracer in to the model. In the parameter studies,  $L$  is varied between 100 m and 10000 km to represent emissions along a narrow coastal strip to an entire continent.

Based upon diagnosis of  $H$  and  $H_{\text{MBL}}$  from the MetUM simulation (Fig. 7),  $H_{\text{MBL}}$  in the box-model is held constant and  $H$  varies sinusoidally between a maximum,  $H_{\text{max}}$ , at 15:00 LT and a minimum (50 m) at 03:00 LT. The residual layer extends from the top of the marine or continental boundary layers ( $H_{\text{MBL}}$  and  $H$  respectively) to the maximum height the continental boundary layer ( $H_{\text{max}}$ ) as described earlier. The residual layer represents the layer of air between the current boundary layer height and the maximum height through which pollution could have been turbulently mixed on previous days. Coastal outflow in the box-model, i.e. horizontal advection across the coast between  $H_{\text{MBL}}$  and  $H_{\text{max}}$  is represented by tracer transport into box-4.

The equations governing the rate of change of tracer mass  $M_1$  to  $M_6$  in each of the boxes are derived from integrating the general tracer conservation equation:

$$\frac{\partial(\rho q)}{\partial t} + \nabla \cdot (\rho q \mathbf{u}) = \rho s - \frac{\rho q}{\alpha} \quad (1)$$

where  $q$  is tracer mixing ratio,  $\rho$  is air density,  $t$  is time,  $\mathbf{u}$  is the 3-D wind vector,  $s$  represents sources (per unit mass) and  $\alpha$  is a loss timescale. Integrating over an arbitrary volume and using Gauss' theorem gives:

$$\frac{d}{dt} \iiint \rho q dV + \iint \rho q (\mathbf{u} - \mathbf{u}_b) \cdot \mathbf{n} dS = \iiint \rho \left( s - \frac{q}{\alpha} \right) dV \quad (2)$$

5 where  $\mathbf{u}_b$  is the velocity of the boundary of the volume and  $\mathbf{n}$  is the outward pointing normal to the boundary. Now assume without loss of generality that the volume is a cuboid with length  $Y$  along the coast, with depth  $H$  and width  $L$  in the cross-coastal direction. Further assume that the lateral boundaries do not move ( $\mathbf{u}_b = 0$ ), but the top boundary can move. It can then be shown that:

$$10 \frac{dM}{dt} = \langle \rho q u \rangle_{in} YH - \langle \rho q u \rangle_{out} YH + \left[ \rho q \frac{dH}{dt} \right] LY + S - \frac{M}{\alpha} \quad (3)$$

where  $M$  is the total tracer mass in the box, the angle-brackets represent averages across the inflow and outflow lateral boundaries of the box and the square brackets denote an average across the top boundary. Note that only the cross-coastal component of the flow has been included for simplicity, but the other components could readily  
15 be included.  $dH/dt$  is the rate of movement of the box top and  $S$  is the box-integrated source rate. This expression is exact and depends only on the definition of the volumes and tracer conservation.

Now some simplifying assumptions are made. The horizontal velocity is assumed to be uniform and the tracer mixing ratio and density at an outflow boundary are assumed  
20 to equal the average throughout the box,  $\langle \rho q \rangle$ . Therefore,

$$\langle \rho q u \rangle_{out} YH = U \langle \rho q \rangle YH = \frac{U}{L} M \quad (4)$$

using  $M = \langle \rho q \rangle LYH$ . Now consider box-1 describing the continental BL where  $M_1 = \langle \rho q \rangle_1 LYH$  and  $H$  is BL height. The tracer inflow is assumed to be zero. If the BL top

Coastal outflow

D. L. Peake et al.

Title Page

Abstract

Introduction

Conclusions

References

Tables

Figures

◀

▶

◀

▶

Back

Close

Full Screen / Esc

Printer-friendly Version

Interactive Discussion



is descending it is assumed that air from the BL is continuously redefined as residual-layer air and has the mixing ratio and density of the average within the BL. Conversely, if the BL top is ascending it is assumed that the BL entrains air with the current mixing ratio and density of the residual layer,  $\langle \rho q \rangle_3$ . Using (Eq. 3) and  $M_3 = \langle \rho q \rangle_3 LY (H_{\max} - H)$  and introducing the normalised BL height  $h = H/H_{\max}$  where  $0 < h < 1$ , the net result for the evolution of mass in box-1 can be written:

$$\frac{dM_1}{dt} = \begin{cases} S - \left(\frac{1}{\alpha}\right) M_1 - \beta M_1 + \frac{1}{1-h} \left(\frac{dh}{dt}\right) M_3; & dH/dt \geq 0 \\ S - \left(\frac{1}{\alpha}\right) M_1 - \beta M_1 + \frac{1}{h} \left(\frac{dh}{dt}\right) M_1; & dH/dt < 0 \end{cases} \quad (5)$$

where the advection rate  $\beta = U/L$ . Similarly for the other two boxes over land we find:

$$\frac{dM_3}{dt} = \begin{cases} -\left(\frac{1}{\alpha}\right) M_3 - \beta M_3 - \frac{1}{1-h} \left(\frac{dh}{dt}\right) M_3; & dH/dt \geq 0 \\ -\left(\frac{1}{\alpha}\right) M_3 - \beta M_3 - \frac{1}{h} \left(\frac{dh}{dt}\right) M_1; & dH/dt < 0 \end{cases} \quad (6)$$

$$\frac{dM_5}{dt} = -\left(\frac{1}{\alpha}\right) M_5 - \beta M_5 \quad (7)$$

The tracer mass crossing the coast into the coastal outflow layer and marine boundary layer depends upon the ratio of the height of the residual layer to the marine boundary layer height,  $\gamma = H_{\max}/H_{\text{MBL}}$ , typically greater than 1. In addition, since the mixing ratio in the continental boundary layer (box-1) is generally greater than in the residual layer above it (box-3), another important parameter is the normalised BL height,  $h$ . The outgoing tracer from the box is assumed to be zero (i.e., it decays before it can leave by advection). The resulting equations for the boxes over ocean are:

$$\frac{dM_2}{dt} = \begin{cases} -\left(\frac{1}{\alpha}\right) M_2 + \left(\frac{1}{\gamma h}\right) \beta M_1; & H \geq H_{\text{MBL}} \\ -\left(\frac{1}{\alpha}\right) M_2 + \beta M_1 + \left(\frac{1-\gamma h}{\gamma-\gamma h}\right) \beta M_3; & H < H_{\text{MBL}} \end{cases} \quad (8)$$

$$\frac{dM_4}{dt} = \begin{cases} -\left(\frac{1}{\alpha}\right) M_4 + \left(1 - \frac{1}{\gamma h}\right) \beta M_1 + \beta M_3; & H \geq H_{\text{MBL}} \\ -\left(\frac{1}{\alpha}\right) M_4 + \left(\frac{\gamma-1}{\gamma-\gamma h}\right) \beta M_3; & H < H_{\text{MBL}} \end{cases} \quad (9)$$

Title Page

Abstract

Introduction

Conclusions

References

Tables

Figures

⏪

⏩

◀

▶

Back

Close

Full Screen / Esc

Printer-friendly Version

Interactive Discussion



$$\frac{dM_6}{dt} = -\left(\frac{1}{\alpha}\right)M_6 + \beta M_5 \quad (10)$$

Equations (5)–(10) are six coupled ordinary differential equations. The continental BL height,  $H$ , is prescribed as a sinusoidally varying function. This introduces switches into the equations due to the conditional statements, making them nonlinear. If the parameters  $\alpha$ ,  $\beta$ ,  $H_{\max}$ ,  $\gamma$  and  $S$  are all taken as constants, analytic solution is possible, as shown in the Appendix. However, since time varying winds ( $\beta$ ) will be used as input, the results presented in all plots were obtained using numerical integration a simple finite difference scheme with 600 s timestep was used (but the results are not sensitive to the scheme chosen). The model is initialised with zero tracer. The source rate of tracer was arbitrarily chosen as unity, as the tracer mass in each box simply scales with  $\alpha S$  (see Appendix).

There are 3 timescales in the problem: the length of day (controlling variation in  $h$ ),  $\alpha$  and  $1/\beta$ . The first is used to scale the time dimension, leaving only 3 non-dimensional parameters plus the sinusoidally varying non-dimensional boundary layer height,  $h$ , controlling the solutions (see Appendix for details). In the following exploration of outflow regimes, the parameters are varied as follows:

- *e-folding tracer lifetime*,  $\alpha$ :  $\alpha$  is varied between 600 s and 32 days, representing a wide range of potential airborne pollutant lifetimes.
- *Advection rate*,  $\beta$ : the  $\beta = U/L$ , where  $U$  is the wind speed ( $\text{ms}^{-1}$ ) and  $L$  is the landwidth (m). The advection rate is proportional to the mass of tracer advected horizontally from the land to sea boxes per second.  $\beta$  is varied from  $10^{-3} \text{ day}^{-1}$  (e.g.,  $U = 0.1 \text{ ms}^{-1}$  and  $L = 10000 \text{ km}$ ) to  $100 \text{ day}^{-1}$  (e.g.,  $U = 10 \text{ ms}^{-1}$  and  $L = 100 \text{ m}$ ).
- *Boundary layer ratio*,  $\gamma$ :  $\gamma = H_{\max}/H_{\text{MBL}}$  is the ratio between the maximum continental boundary layer height and the marine boundary layer height. If  $\gamma = 1$  then there is no coastal outflow layer. In the MetUM simulation, with the parameters

Coastal outflow

D. L. Peake et al.

Title Page	
Abstract	Introduction
Conclusions	References
Tables	Figures
◀	▶
◀	▶
Back	Close
Full Screen / Esc	
Printer-friendly Version	
Interactive Discussion	



## Coastal outflow

D. L. Peake et al.

Title Page

Abstract

Introduction

Conclusions

References

Tables

Figures



Back

Close

Full Screen / Esc

Printer-friendly Version

Interactive Discussion



$H_{\max} = 2000$  m and  $H_{\text{MBL}} = 400$  m did not vary greatly and so  $\gamma \approx 5$ . In the parameter study,  $\gamma$  is varied from 1 to 7 based upon observations from studies that observed typical MBL depths of up to 250 to 750 m in the Gulf of Maine (Angevine et al., 2006; Wolfe et al., 2007).

An important combination of parameters  $\alpha\beta$  describes the decay rate of tracers relative to the advection rate and has a major influence on the solutions. When  $\alpha\beta = 1$ , tracer decay and advection rates are equal, thus it takes one tracer lifetime for tracer to be advected a distance equal to one landwidth. When  $\alpha\beta > 10$ , the tracer is *long-lived* relative to the advection timescale. When  $\alpha\beta < 0.1$ , the tracer is described as *short-lived*.

## 4.2 Exploring parameter regimes of coastal outflow

Figure 8a shows the diurnally averaged tracer amount (as the proportion of total domain tracer) within the coastal outflow box (box-4) as a function of tracer decay rate and advection rate using a constant BL-ratio  $\gamma = 5$ . As the decay rate decreases the proportion of tracer in the coastal outflow layer increases. The increased lifetime of the tracer enables it to undergo greater horizontal advection before it decays to small values, and thus has greater potential to be exported across the coast. Decreasing the decay rate by three orders of magnitude increases the percentage of tracer in the coastal outflow box from 1 % to 70 % (for a fixed advection rate of  $1 \text{ day}^{-1}$ ).

As the advection rate increases from the short-lived regime ( $\alpha\beta < 1$ ) the proportion of tracer undergoing coastal outflow also increases, consistent with the idea that a greater cross-coastal wind speed allows greater advection and thus greater chance of tracer export across the coast. However, increasing advection rate too far results in a decrease in coastal outflow. This occurs because the advection rate becomes so large that tracer advected horizontally out of the continental residual layer during the night-time, is not replenished in the residual layer until the  $H$  increases in depth the next day. This reduces the availability of tracer available to undergo coastal outflow.

## Coastal outflow

D. L. Peake et al.

Title Page

Abstract

Introduction

Conclusions

References

Tables

Figures



Back

Close

Full Screen / Esc

Printer-friendly Version

Interactive Discussion



The dependence on daylength is most obvious for the tracers with slowest decay rate, where the maximum in the outflow layer occurs for an advection rate of  $1 \text{ day}^{-1}$ . For tracers with faster decay, the maximum occurs for  $\alpha\beta \approx 10$ .

The variation of the diurnally averaged proportion of tracer in the coastal outflow layer with changes in  $\alpha\beta$  and  $\gamma$  is shown in Fig. 8b. For short-lived tracers ( $\alpha\beta < 1$ ) the proportion of tracer undergoing coastal outflow is almost independent of the BL-ratio, however for long-lived tracers ( $\alpha\beta > 1$ ) the proportion of tracer undergoing coastal outflow depends on the BL-ratio,  $\gamma$ . As  $\gamma$  increases, the proportion of tracer in the coastal outflow layer increases due to the change in proportion of time that  $H > H_{\text{MBL}}$  in the box-model. However, given the relatively small range of BL-ratio ( $3 < \gamma < 6$ ) exhibited in the MetUM simulation, and the small impact that variation in BL-ratio produces in coastal outflow, it can be concluded that synoptic variations in BL-ratio are relatively unimportant in determining the day-to-day variability in coastal outflow amount.

The mass of tracer in the continental residual tracer, as a proportion of all tracer over the land (i.e.  $M_3/(M_1 + M_3)$ ), is shown in Fig. 8c for  $\gamma = 5$ . The maximum percentage of tracer in the continental residual layer is 50% in the diurnal average due to the sinusoidal variation in  $H$  between 50 m ( $h \approx 0$ ) and  $H = H_{\text{max}}$  ( $h = 1$ ) within the box-model. For short-lived tracers ( $\alpha\beta < 0.1$ ) the proportion of mass within the continental residual layer is dependent only on the tracer decay rate, with less surviving in the residual layer for faster decay. For long-lived tracers ( $\alpha\beta > 10$ ) the proportion within the continental residual layer is dependent only on the advection rate; increasing the advection rate depletes the proportion of long-lived tracer over land within the continental residual layer and causes the subsequent reduction of coastal outflow, which can also be seen in Fig. 8a and b.

The diurnal variability of tracer in the coastal outflow box is defined as the range over 24 h divided by its diurnal average. Figure 8d shows the diurnal variability for a BL-ratio of  $\gamma = 5$ . For short-lived tracers ( $\alpha\beta < 0.1$ ) the diurnal variability is independent of the advection rate and entirely dependent on the lifetime of the tracer. As the lifetime of the



[Title Page](#)[Abstract](#)[Introduction](#)[Conclusions](#)[References](#)[Tables](#)[Figures](#)[Back](#)[Close](#)[Full Screen / Esc](#)[Printer-friendly Version](#)[Interactive Discussion](#)

difference between the models is small. A sensitive diagnostic is to calculate the correlation divided by the RMS difference, as shown in Fig. 9 for a fixed tracer lifetime of 1 day. A maximum in correlation divided by difference occurs at  $\beta = 2 \text{ day}^{-1}$ . Thus, given an average 850 hPa cross-coastal wind speed of  $U = 2.14 \text{ ms}^{-1}$  (based on the MetUM simulation), the representative landwidth,  $L = U/\beta$  is approximately 100 km. Note that the diurnal cycle is relatively insensitive to  $\gamma$ , but the best fit is obtained when using  $\gamma = 4$  which is close to the value obtained from the boundary layer in the mesoscale model.

## 5.2 Representing day-to-day variability

An alternative method for estimating the representative landwidth is to compare longer timescale variability in the tracer mass in the coastal outflow box predicted by the simple box model with the time series calculated from the realistic mesoscale model simulation. In particular, the diurnal cycle has been filtered out to focus on synoptic timescale variability. In order to carry out this comparison it is necessary to force the box-model using the time varying cross-coastal windspeed from the MetUM simulation. The cross-coastal wind speed was calculated along the coastline shown in thick black in Fig. 1, with an average heading of  $30^\circ \text{ N}$ . The 850 hPa pressure level occurs at a height within the coastal outflow layer based upon the boundary layer heights calculated from the MetUM. The 850 hPa cross-coastal wind speed is on average  $U = 2.14 \text{ ms}^{-1}$ . A running median filter with 24 h window is used to remove the diurnal cycle from the hourly mesoscale model output. The standard deviation of the cross-coastal time-filtered winds is  $\sigma = 1.49 \text{ ms}^{-1}$ .

The filtered time series of cross-coastal wind was fed into the box model run using fixed parameters  $\alpha = 1 \text{ day}$ ,  $\gamma = 5$  and a value for landwidth,  $L$ , used to find  $\beta = U/L$ . The resulting output was also passed through the 24 h filter. The box model was re-run with different values of  $L$ . This fixes the width of the domain experiencing emissions. The amount of tracer in the coastal outflow box ( $M_4$ ) depends on the amount of tracer over land ( $M_L$ ) which in turn depends on  $L$  (Eqs. 5–9). We find that a landwidth of

## Coastal outflow

D. L. Peake et al.

Title Page

Abstract

Introduction

Conclusions

References

Tables

Figures

◀

▶

◀

▶

Back

Close

Full Screen / Esc

Printer-friendly Version

Interactive Discussion



approximately 400 km gives box-model results that match the MetUM simulation most closely. Figure 10 shows 24 h running averages of coastal outflow from both models. The box-model is able to capture the major episodes of coastal outflow, with the proportion of tracer in the coastal outflow exhibiting a similar variation to that shown in the MetUM. The correlation between the percentage of tracer in the coastal outflow box in the MetUM and box-model simulations is +0.69, which implies that the variability in the cross-coastal windspeed accounts for 48 % of the variance in coastal outflow. For some periods, the box-model does not capture the variability in MetUM simulated coastal outflow. This is likely to be due to weak synoptically forced situations when mesoscale circulations, such as shallow convection and sea breeze circulations, can ventilate tracer from the continental boundary layer. These mesoscale circulations are not represented in the box-model, but are represented in the MetUM as discussed in Sect. 2.

## 6 Conclusions

In this paper the magnitude and variability of coastal outflow is quantified using the MetUM and a simple box-model. The MetUM showed that over a 4 week period in summer 2004, horizontal ventilation of the continental boundary layer by coastal outflow was similar to the magnitude by vertical ventilation by convective and vertical advection for the whole of the eastern USA.

The regional tracer mass budget was reduced to a box-model describing coastal outflow using only three parameters; the tracer lifetime, cross-coastal wind speed, and ratio of  $H_{\max}$  to  $H_{\text{MBL}}$ . The least important variable in controlling the proportion of tracer in the coastal outflow layer from day to day was  $H_{\max}$ , although its diurnal cycle was instrumental in producing diurnal cycles in coastal outflow for short-lived tracers.

A non-dimensional ratio ( $\alpha\beta$ ) is defined by dividing the advection rate by the decay rate. Short-lived ( $\alpha\beta < 0.1$ ) and long-lived ( $\alpha\beta > 10$ ) tracers exhibit different coastal outflow dependencies. For short-lived tracers, increasing the advection rate increases

the magnitude of coastal outflow. For long-lived tracers increasing the advection rate decreases the magnitude of coastal outflow, due to reduced availability of tracer, and increases the diurnal variability of coastal outflow.

By varying the few parameters of the box model, it is argued that the parameter values that obtain the best fit relative to the mesoscale model simulation are relevant to the transport regime across the eastern USA. In particular, the *representative land-width* is obtained as the value that best explains variability in the pollutant loading in the coastal outflow layer. When considering the composite diurnal cycle a relatively short landwidth of 100–200 km was found to be capable of explaining the average range of the diurnal variation. However, for synoptic timescale variability (after applying a running mean filter with 24 h window) a landwidth of 400 km was found to describe best the observed variability. The results imply that coastal outflow has a strong influence on regional pollution across the region for a considerable distance from the coast.

## Appendix A

### Analytical solutions for the box model

The box model Eqs. (5)–(10) can be solved analytically if the parameters  $\alpha$ ,  $\beta$ ,  $H_{\max}$ ,  $\gamma$  and  $S$  are all taken as constant. In doing so, it is most convenient to recast them in the non-dimensional form:

$$\dot{m}_1 = \begin{cases} 1 - (1 + \lambda)m_1 + \frac{\dot{h}}{1-\dot{h}}m_3 & \dot{h} \geq 0 \\ 1 - \left(1 + \lambda - \frac{\dot{h}}{h}\right)m_1 & \dot{h} < 0 \end{cases} \quad (\text{A1})$$

$$\dot{m}_3 = \begin{cases} -\left(1 + \lambda + \frac{\dot{h}}{1-\dot{h}}\right)m_3 & \dot{h} \geq 0 \\ -(1 + \lambda)m_3 - \left(\frac{\dot{h}}{h}\right)m_1 & \dot{h} < 0 \end{cases} \quad (\text{A2})$$

[Title Page](#)[Abstract](#)[Introduction](#)[Conclusions](#)[References](#)[Tables](#)[Figures](#)[⏪](#)[⏩](#)[◀](#)[▶](#)[Back](#)[Close](#)[Full Screen / Esc](#)[Printer-friendly Version](#)[Interactive Discussion](#)

$$\dot{m}_2 = \begin{cases} -m_2 + \lambda \left(\frac{h_m}{h}\right) m_1 & h \geq h_m \\ -m_2 + \lambda m_1 + \lambda \left(\frac{h_m - h}{1 - h}\right) m_3 & h < h_m \end{cases} \quad (\text{A3})$$

$$\dot{m}_4 = \begin{cases} -m_4 + \lambda \left(1 - \frac{h_m}{h}\right) m_1 + \lambda m_3 & h \geq h_m \\ -m_4 + \lambda \left(\frac{1 - h_m}{1 - h}\right) m_3 & h < h_m \end{cases} \quad (\text{A4})$$

$$\dot{m}_5 = -(1 + \lambda) m_5 \quad (\text{A5})$$

$$\dot{m}_6 = -m_6 + \lambda m_5 \quad (\text{A6})$$

In Eqs. (A1)–(A6) time, length and mass have been non-dimensionalised so that  $\hat{t} = t/\alpha$ ,  $h = H/H_{\max}$ ,  $m_i = M_i/(\alpha S)$  and  $\dot{m}_1$  denotes the derivative with respect to  $\hat{t}$  and so on. There are then only two constant non-dimensional parameters  $\lambda \equiv \alpha\beta$  and  $h_m \equiv H_{\text{MBL}}/H_{\max} \equiv 1/\gamma$  plus the sinusoidally varying boundary layer height,  $h$ . Note that in this particular scaling of time, the length of day  $\hat{t}_d = t_d/\alpha$  where  $t_d$  is the dimensional day length.

These coupled first order ODEs can be solved by judicious inspection of the nature of the coupling and the conditional switches. The equation for  $m_5$  is decoupled from the rest of the system and so  $m_5$  can be easily solved first. The solution can then be plugged into the last equation to solve for  $m_6$ :

$$m_5(t) = m_5(0)e^{-(1+\lambda)t} \quad (\text{A7})$$

$$m_6(t) = m_6(0)e^{-t} + m_5(0)e^{-t}(1 - e^{-\lambda t}) \quad (\text{A8})$$

With the specified initial conditions,  $m_i(t) = 0$ ,  $\forall i$ , we get  $m_5(t) = m_6(t) = 0$ ,  $\forall t$ ; hence, boxes 5 and 6 play no role and we effectively have a 4-box model.

The equations for  $m_1$  and  $m_3$  are coupled to each other, and those for  $m_2$  and  $m_4$  are mutually coupled as well as to those for  $m_1$  and  $m_3$ . Hence, it is sensible to attempt to solve for  $m_1$  and  $m_3$  first, followed by  $m_2$  and  $m_4$ . Three unconditional equations can be obtained by adding the above equations for the total mass  $m = m_1 + m_2 + m_3 + m_4 +$

$m_5 + m_6$ , the sum of the mass in boxes 1 and 3,  $m_{13} \equiv m_1 + m_3$  and the sum of mass in boxes 2 and 4,  $m_{24} \equiv m_2 + m_4$ :

$$\dot{m} = 1 - m \quad (\text{A9})$$

$$\dot{m}_{13} = 1 - (1 + \lambda)m_{13} \quad (\text{A10})$$

$$5 \quad \dot{m}_{24} = -m_{24} + \lambda m_{13} \quad (\text{A11})$$

The solution of Eq. (A9) for the total mass is

$$m(t) = m(0)e^{-t} + (1 - e^{-t}) \quad (\text{A12})$$

10 This solution shows that, irrespective of the initial mass  $m(0)$  in the system, the steady state mass is given by  $m(\infty) = 1$ , i.e.  $M(\infty) = \alpha S$ , the amount of material emitted in a time equal to the tracer lifetime  $\alpha$ , and is independent of  $\beta$ .

Equation (A10) integrates to give:

$$m_{13}(t) = m_{13}(0)e^{-(1+\lambda)t} + \frac{1}{1+\lambda}(1 - e^{-(1+\lambda)t}) \quad (\text{A13})$$

which can be used with Eq. (A11) to give

$$15 \quad m_{24}(t) = m_{24}(0)e^{-t} + \left( m_{13}(0) - \frac{1}{1+\lambda} \right) (e^{-t} - e^{-(1+\lambda)t}) + \frac{\lambda}{1+\lambda} (1 - e^{-t}) \quad (\text{A14})$$

In the asymptotic limit  $t \rightarrow \infty$  we find that  $m_{13}(\infty) = 1/(1 + \lambda)$  and  $m_{24}(\infty) = \lambda/(1 + \lambda)$ , so that the proportion of mass over sea is a factor of  $\alpha\beta$  times that over land at steady state.

20 The above solutions hold for all time  $t$ . The individual form of the solutions for  $m_1$  and  $m_3$  will depend on the sign of  $\dot{h}$  and, for  $m_2$  and  $m_4$ , additionally on the sign of  $h - h_m$ . The solutions for  $m_1$  and  $m_3$  are given by

$$m_1(t) = \begin{cases} \left[ m_1(0) + m_3(0) \frac{h(t)-h(0)}{1-h(0)} \right] e^{-(1+\lambda)t} + \frac{1}{1+\lambda} [1 - e^{-(1+\lambda)t}], & \dot{h} \geq 0 \\ m_1(0) \frac{h(t)}{h(0)} e^{-(1+\lambda)t} + h(t) \int_0^t \frac{e^{(1+\lambda)(s-t)}}{h(s)} ds, & \dot{h} < 0 \end{cases} \quad (\text{A15})$$

10876

Title Page

Abstract

Introduction

Conclusions

References

Tables

Figures

⏪

⏩

◀

▶

Back

Close

Full Screen / Esc

Printer-friendly Version

Interactive Discussion



$$m_3(t) = \begin{cases} m_3(0) \frac{h(t)-1}{h(0)-1} e^{-(1+\lambda)t}, & \dot{h} \geq 0 \\ \left[ m_3(0) + m_1(0) \frac{h(0)-h(t)}{h(0)} \right] e^{-(1+\lambda)t} \\ + \frac{1}{1+\lambda} [1 - e^{-(1+\lambda)t}] - h(t) \int_0^t \frac{e^{(1+\lambda)(s-t)}}{h(s)} ds, & \dot{h} < 0 \end{cases} \quad (\text{A16})$$

Note that here the zero point of time is taken as the last time switching between  $\dot{h} \geq 0$  and  $\dot{h} < 0$  occurred, so that  $m_1(0), m_3(0)$  and  $h(0)$  each refers to the end value obtained from the previous solution. The residual integral in Eqs. (A15) and (A16) can be computed numerically for known  $h(t)$ . Assuming a sinusoidally varying boundary layer height, we may write  $h(t) = \epsilon \sin(\omega t) + (1 - \epsilon)$ , where  $\epsilon = (1 - h_{\min})/2$ ,  $\omega = 2\pi/\hat{t}_d$  and  $\hat{t}_d = t_d/\alpha$ , where  $t_d$  is the length of day.

From Eqs. (A3) and (A4) the solutions for  $m_2$  and  $m_4$  can be written formally as

$$m_2 = m_2(0)e^{-t} + \lambda h_m \int_0^t \frac{e^{s-t} m_1(s)}{h(s)} ds \quad h \geq h_m \quad (\text{A17})$$

$$m_4 = m_4(0)e^{-t} + \lambda(1 - h_m) \int_0^t \frac{e^{s-t} m_3(s)}{1 - h(s)} ds \quad h < h_m \quad (\text{A18})$$

with the corresponding solutions of  $m_2$  for  $h < h_m$  and  $m_4$  for  $h \geq h_m$  obtained by subtraction from the solution of  $m_{24}$ , Eq. (A14). Substitution of the solutions for  $m_1$  and  $m_3$  into Eqs. (A17) and (A18) include terms with residual integrals that cannot be evaluated explicitly but that can be readily computed by numerical quadrature, e.g. using Simpson's rule.

*Acknowledgements.* The authors would like to thank the Met Office for use of their Unified Model and Willie McGinty for his help running the Unified Model. We also thank Bob Plant, Janet Barlow, Sue Gray and Jane Lewis for useful comments on this work. Dan Peake was supported by a NERC PhD studentship. The NOAA-DOE radar wind profiler data was obtained

Coastal outflow

D. L. Peake et al.

Title Page

Abstract

Introduction

Conclusions

References

Tables

Figures

◀

▶

◀

▶

Back

Close

Full Screen / Esc

Printer-friendly Version

Interactive Discussion



via the NOAA ESRL (Earth System Research Laboratory) database (<http://www.esrl.noaa.gov/psd/data/obs/datadisply/>) and the EPA (Environmental Protection Agency) CO data from <http://www.epa.gov/ttnairs1/airsaqs-o/detaildata/downloadaqsdata.htm>.

## References

- 5 Angevine, W. M., Hare, J. E., Fairall, C. W., Wolfe, D. E., Hill, R. J., Brewer, W. A., and White, A. B.: Structure and formation of the highly stable marine boundary layer over the Gulf of Maine, *J. Geophys. Res.*, 111, D23S22, doi:10.1029/2006JD007465, 2006. 10856, 10869
- 10 Carter, D. A., Gage, K. S., Ecklund, W. L., Angevine, W. M., Johnston, P. E., Riddle, A. C., Wilson, J., and Williams, C. R.: Developments in UHF lower tropospheric wind profiling technology at NOAA's Aeronomy Laboratory, *Radio Sci.*, 30, 997–1001, 1995. 10858
- Dacre, H. F., Gray, S. L., and Belcher, S. E.: A case study of boundary layer ventilation by convection and coastal processes, *J. Geophys. Res.*, 112, D17106, doi:10.1029/2006JD007984, 2007. 10855
- 15 Davis, S. R., Talbot, R., and Mao, H.: Transport and outflow to the North Atlantic in the lower marine troposphere during ICARTT 2004, *Atmos. Chem. Phys. Discuss.*, 12, 2395–2434, doi:10.5194/acpd-12-2395-2012, 2012. 10856
- Dickerson, R. R., Rhoads, K. P., Carsey, T. P., Oltmans, S. J., Burrows, J. P., and Crutzen, P. J.: Ozone in the remote marine boundary layer: a possible role for halogens, *J. Geophys. Res.*, 20 104, 21385–21395, 1999. 10856
- Fehsenfeld, F. C., Ancellet, G., Bates, T. S., Goldstein, A. H., Hardesty, R. M., Honrath, R., Law, K. S., Lewis, A. C., Leaitch, R., McKeen, S., Meagher, J., Parrish, D. D., Pszenny, A. A. P., Russel, P. B., Schlager, H., Seinfeld, J., Talbot, R., and Zbinden, R.: International Consortium for Atmospheric Research on Transport and Transormation (ICARTT): 25 North America to Europe – overview of the 2004 summer field study, *J. Geophys. Res.*, 111, D23S01, doi:10.1029/2006JD007829, 2006. 10855, 10858
- Holzer, M. and Hall, T. M.: Low-level transpacific transport, *J. Geophys. Res.*, 112, D09103, doi:10.1029/2006JD007828, 2007. 10856

## Coastal outflow

D. L. Peake et al.

Title Page

Abstract

Introduction

Conclusions

References

Tables

Figures



Back

Close

Full Screen / Esc

Printer-friendly Version

Interactive Discussion



## Coastal outflow

D. L. Peake et al.

[Title Page](#)[Abstract](#)[Introduction](#)[Conclusions](#)[References](#)[Tables](#)[Figures](#)[Back](#)[Close](#)[Full Screen / Esc](#)[Printer-friendly Version](#)[Interactive Discussion](#)

- Lock, A. P., Brown, A. R., Bush, M. R., Martin, G. M., and Smith, R. N. B.: A new boundary layer mixing scheme. Part I: Scheme description and single-column model tests, *Mon. Weather Rev.*, 128, 3187–3199, 2000. 10858
- 5 Methven, J., Arnold, S. R., Stohl, A., Evans, M. J., Avery, M., Law, K., Lewis, A. C., Monks, P. S., Parrish, D. D., Reeves, C. E., Schlager, H., Atlas, E., Blake, D. R., Coe, H., Crosier, J., Flocke, F. M., Holloway, J. S., Hopkins, J. R., McQuaid, J., Purvis, R., Rappenglück, B., Singh, H. B., Watson, N. M., Whalley, L. K., and Williams, P. I.: Establishing Lagrangian connections between observations within air masses crossing the Atlantic during the International Consortium for Atmospheric Research on Transport and Transformation, *J. Geophys. Res.*, 111, D23S62, doi:10.1029/2006JD007540, 2006. 10856
- 10 Müller, D., Franke, K., Wagner, F., Althausen, D., Ansmann, A., Heintzenberg, J., and Verver, G.: Vertical profiling of optical and physical particle properties over the tropical Indian Ocean with six-wavelength lidar 2. Case studies, *J. Geophys. Res.*, 106, 28577–28595, 2001. 10856
- Owen, R. C., Cooper, O. R., Stohl, A., and Honrath, R. E.: An analysis of the mechanisms of North American pollutant transport to the central North Atlantic lower free troposphere, *J. Geophys. Res.*, 111, D23S58, doi:10.1029/2006JD007062, 2006. 10856
- 15 Paluch, I. R., Lenschow, D. H., Hudson, J. G., and Peasron Jr., R.: Transport and mixing processes in the lower Troposphere over the Ocean, *J. Geophys. Res.*, 97, 7527–7541, 1992. 10856
- 20 Skillingstad, E. D., Samelson, R. M., Mahrt, L., and Barbour, P.: A numerical modeling study of warm offshore flow over cool water, *Mon. Weather Rev.*, 133, 345–361, 2005. 10856
- VanCuren, R. A., Cliff, S. S., Perry, K. D., and Jimenez-Cruz, M.: Asian continental aerosol persistence above the marine boundary layer over the eastern North Pacific: continuous aerosol measurements from Intercontinental Transport and Chemical Transformation 2002 (ITCT 2K2), *J. Geophys. Res.*, 110, D09S90, doi:10.1029/2004JD004973, 2005. 10856
- 25 Verma, S., Boucher, O., Venkataraman, C., Reddy, M. S., Müller, D., Chazette, P., and Crouzille, B.: Aerosol lofting from sea breeze during the Indian Ocean Experiment, *J. Geophys. Res.*, 111, D07208, doi:10.1029/2005JD005953, 2006. 10856
- Vickers, D., Mahrt, L., Sun, J., and Crawford, T.: Structure of offshore flow, *Mon. Weather Rev.*, 129, 1251–1258, 2001. 10856
- 30 Wolfe, D. E., Brewer, W. A., Tucker, S. C., White, A. B., White, D. E., Welsh, D. C., Ruffieux, D., Fairall, C. W., Ratterree, M., Intrieri, J. M., McCarty, B. J., and Law, D. C.: Shipboard mul-

Coastal outflow

D. L. Peake et al.

Title Page

Abstract

Introduction

Conclusions

References

Tables

Figures



Back

Close

Full Screen / Esc

Printer-friendly Version

Interactive Discussion



## Coastal outflow

D. L. Peake et al.

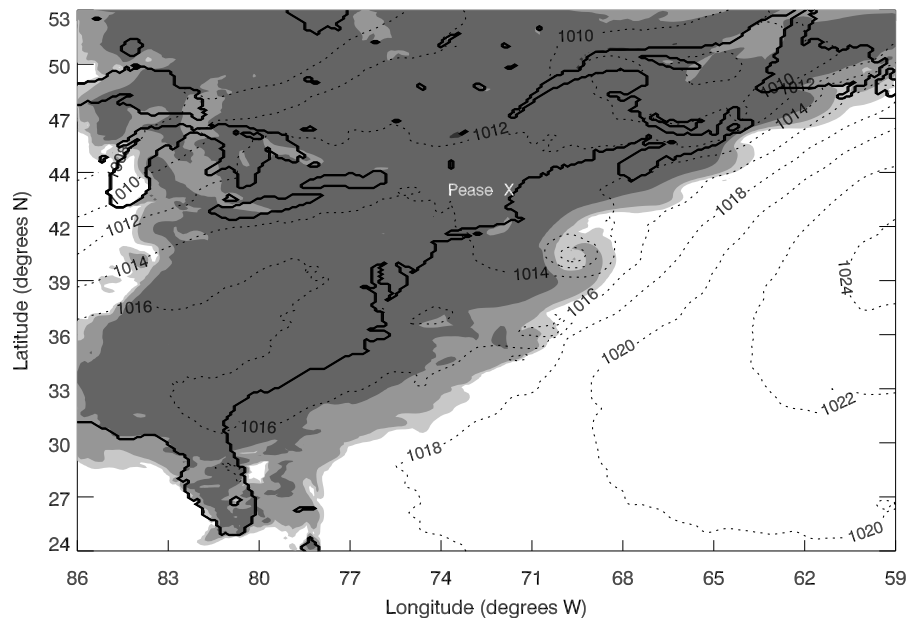


**Fig. 1.** Tracer mixing ratio (shading) at 15:00 UTC on 21 July 2004, 720 m.a.s.l. Each shade represents a change in tracer concentration by a factor of 10 with dark grey representing the highest mixing ratios. Mean sea level pressure (dotted). The cross marks the location of the wind profiler at Pease.

[Title Page](#)[Abstract](#)[Introduction](#)[Conclusions](#)[References](#)[Tables](#)[Figures](#)[◀](#)[▶](#)[◀](#)[▶](#)[Back](#)[Close](#)[Full Screen / Esc](#)[Printer-friendly Version](#)[Interactive Discussion](#)

## Coastal outflow

D. L. Peake et al.

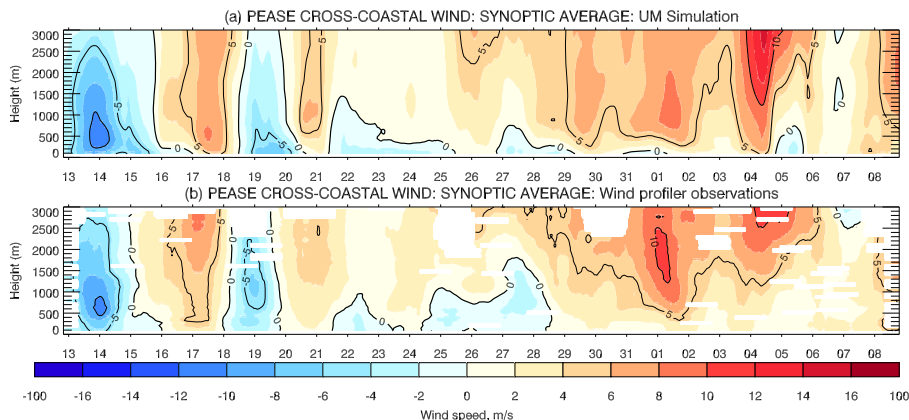


**Fig. 2.** 24 h centred running average of cross-coastal direction wind speed at Pease **(a)** as simulated by the MetUM and **(b)** as observed by 915 MHz wind profiler. The x axis is labelled with the dates in July and August 2004. Positive wind speeds represent off-shore flow and negative wind speeds represent on-shore flow.

[Title Page](#)[Abstract](#)[Introduction](#)[Conclusions](#)[References](#)[Tables](#)[Figures](#)[◀](#)[▶](#)[◀](#)[▶](#)[Back](#)[Close](#)[Full Screen / Esc](#)[Printer-friendly Version](#)[Interactive Discussion](#)

## Coastal outflow

D. L. Peake et al.

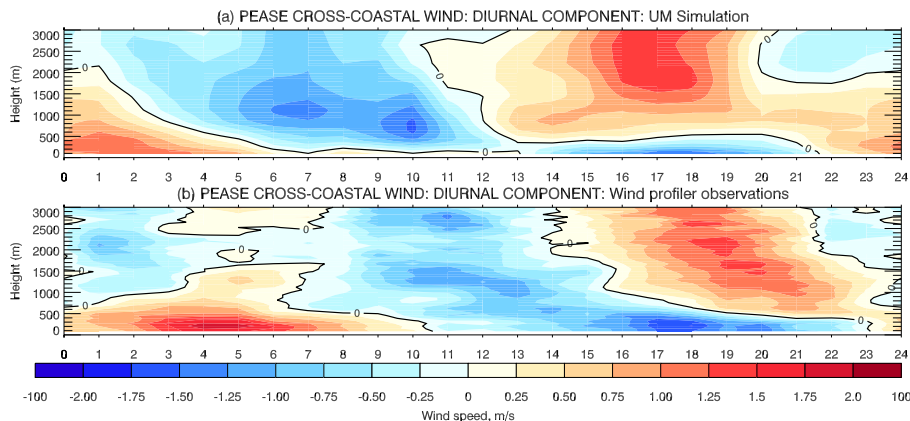


**Fig. 3.** 27 day average diurnal component of cross-coastal direction windspeed at Pease **(a)** as simulated by the MetUM and **(b)** as observed by 915 MHz wind profiler. The  $x$  axis is labelled by the hour in local summer time (UTC – 4). Positive wind speeds represent off-shore flow and negative wind speeds represent on-shore flow.

[Title Page](#)[Abstract](#)[Introduction](#)[Conclusions](#)[References](#)[Tables](#)[Figures](#)[⏪](#)[⏩](#)[⏴](#)[⏵](#)[Back](#)[Close](#)[Full Screen / Esc](#)[Printer-friendly Version](#)[Interactive Discussion](#)

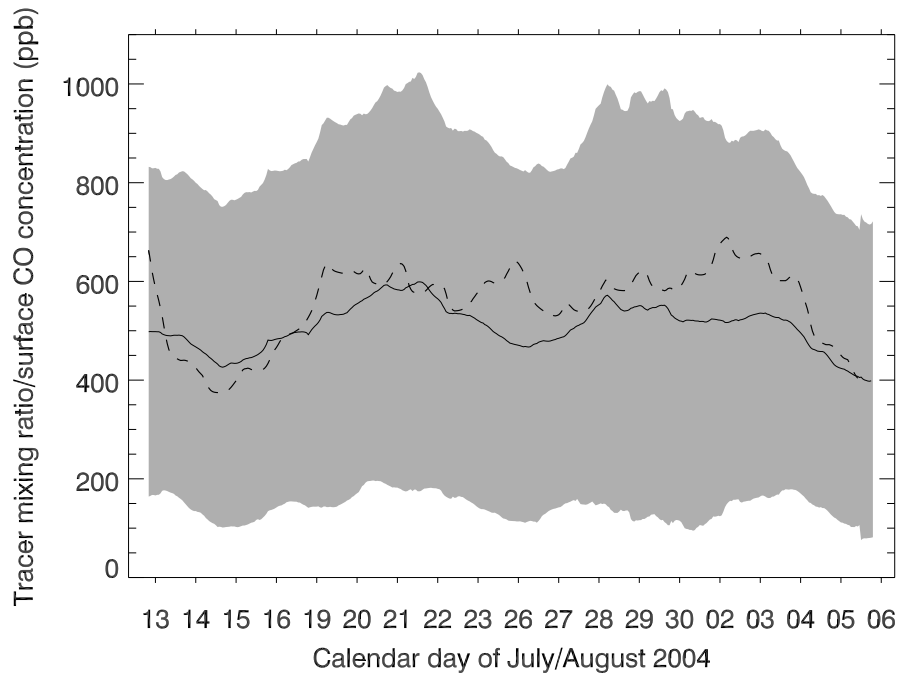


**Fig. 4.** 24 h running average surface CO concentration observations averaged over 121 sites (weekends have been removed). Mean (solid line) plus/minus standard deviation between sites (grey shading). 24 h running average of model tracer mixing ratio within the continental boundary layer (dashed).

Coastal outflow

D. L. Peake et al.

Title Page

Abstract	Introduction
Conclusions	References
Tables	Figures

⏪
⏩

◀
▶

Back	Close
------	-------

Full Screen / Esc

Printer-friendly Version

Interactive Discussion



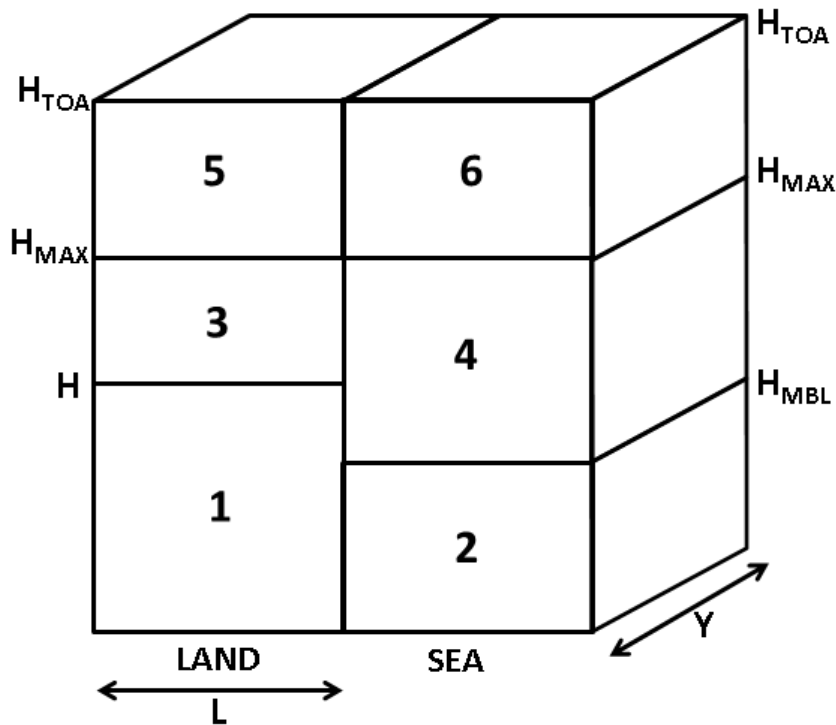


**Fig. 5.** A schematic of the 6-box partition used to analyse tracer transport in the MetUM simulation, which subsequently forms the basis of a box model.  $H$  and  $H_{\text{MBL}}$  are the heights of the continental and marine boundary layers respectively.  $H_{\text{max}}$  is the maximum height of the continental boundary layer, defining the top of the residual layer.  $H_{\text{TOA}}$  represents the top of the atmosphere. Boxes 1, 3 and 5 are over land whilst boxes 2, 4 and 6 are over the sea.  $L$  represents the width of the domain experiencing emissions and  $Y$  represents the length along the coast.

Title Page

Abstract

Introduction

Conclusions

References

Tables

Figures

◀

▶

◀

▶

Back

Close

Full Screen / Esc

Printer-friendly Version

Interactive Discussion



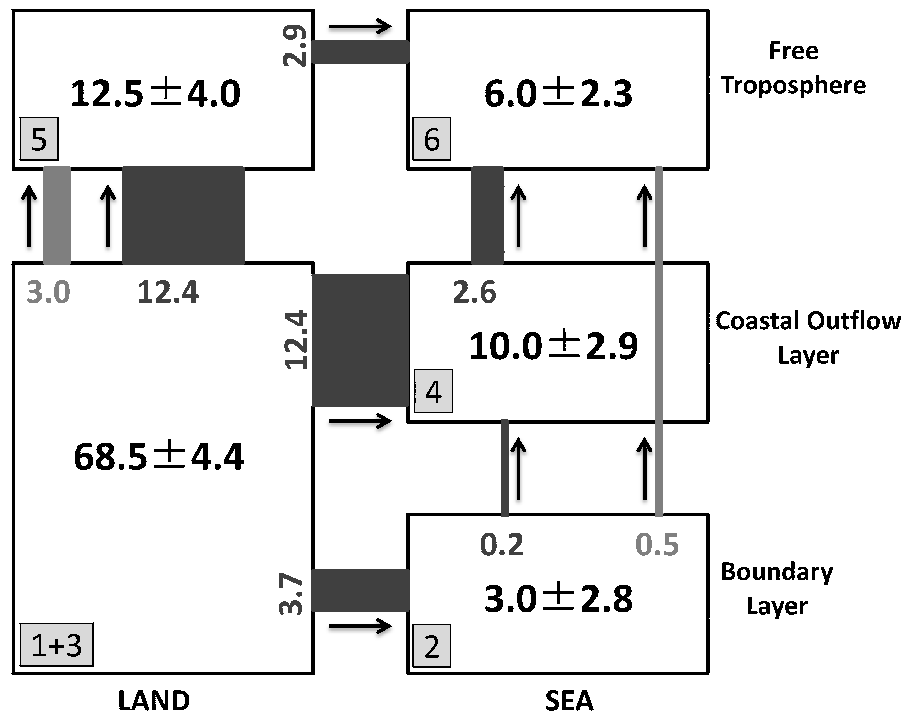


**Fig. 6.** Schematic showing the quasi steady-state distribution of tracer in balance between continuous emission at the land surface and uniform decay with a 24 h lifetime in the MetUM simulation. The continental boundary and residual layers (boxes 1 and 3) are combined into one box. Numbers in the center each box represent the average units of tracer residing in each box, plus/minus one standard deviation, normalised such that the total is 100. The arrows indicate the direction of net mass transport between boxes and the numbers and width of each band represent the amount transported along the related pathway in order to maintain steady state. Light grey arrows are estimates of transport by convection, and dark grey for advection and turbulent mixing.

Title Page

Abstract Introduction

Conclusions References

Tables Figures

◀ ▶

◀ ▶

Back Close

Full Screen / Esc

Printer-friendly Version

Interactive Discussion



## Coastal outflow

D. L. Peake et al.

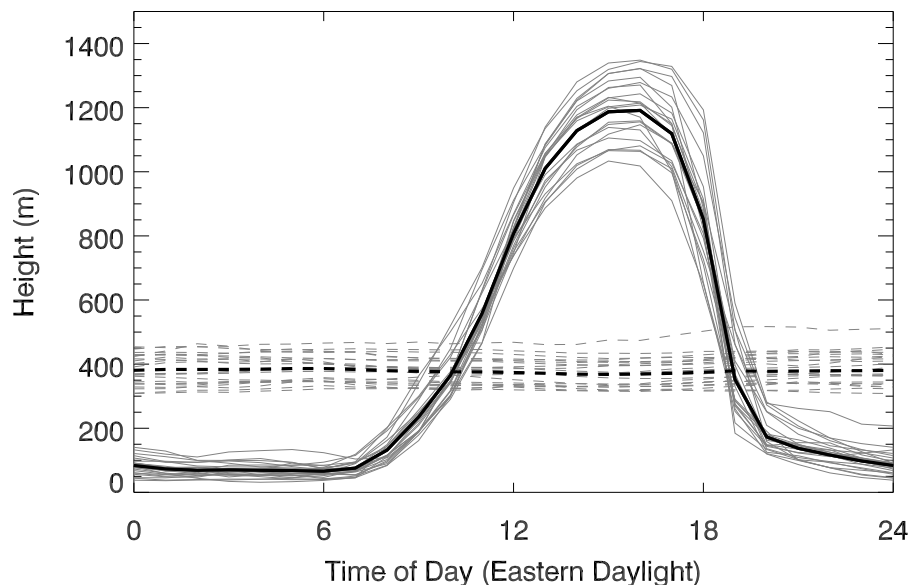


**Fig. 7.** Diurnal cycle in boundary layer heights averaged over the land (solid lines) and sea (dashed lines) for the MetUM simulation. Individual grey lines represent different days of the MetUM simulation, the thick black lines represent the mean boundary layer height cycles. Time is presented with respect to Eastern Daylight Time (UTC – 4).

[Title Page](#)[Abstract](#)[Introduction](#)[Conclusions](#)[References](#)[Tables](#)[Figures](#)[◀](#)[▶](#)[◀](#)[▶](#)[Back](#)[Close](#)[Full Screen / Esc](#)[Printer-friendly Version](#)[Interactive Discussion](#)

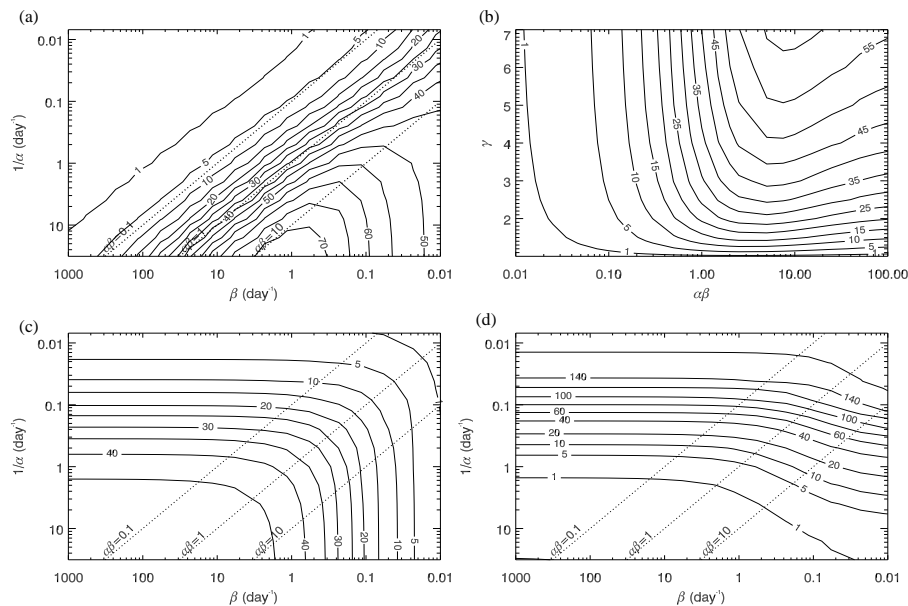


**Fig. 8.** (a) Diurnally averaged tracer in the coastal outflow box (percentage of total domain tracer) as a function of decay rate  $1/\alpha$  and advection rate  $\beta$ . (b) Diurnally averaged percentage of tracer in the coastal outflow layer as a function of  $\alpha\beta$  and BL-ratio  $\gamma$  for  $\alpha = 1$  day. (c) Diurnal average of tracer in the residual layer above land ( $M_3/(M_1 + M_3)$ ) as a function of  $1/\alpha$  and  $\beta$ . (d) Diurnal variability of tracer (diurnal range divided by diurnal mean) as a function of  $1/\alpha$  and  $\beta$ . In (a), (c) and (d) the BL-ratio is constant,  $\gamma = 5$ . Long-lived tracers are represented by  $\alpha\beta > 10$ , short-lived tracers are represented by  $\alpha\beta < 0.1$ .

[Title Page](#)
[Abstract](#)
[Introduction](#)
[Conclusions](#)
[References](#)
[Tables](#)
[Figures](#)
[Back](#)
[Close](#)
[Full Screen / Esc](#)
[Printer-friendly Version](#)
[Interactive Discussion](#)


## Coastal outflow

D. L. Peake et al.

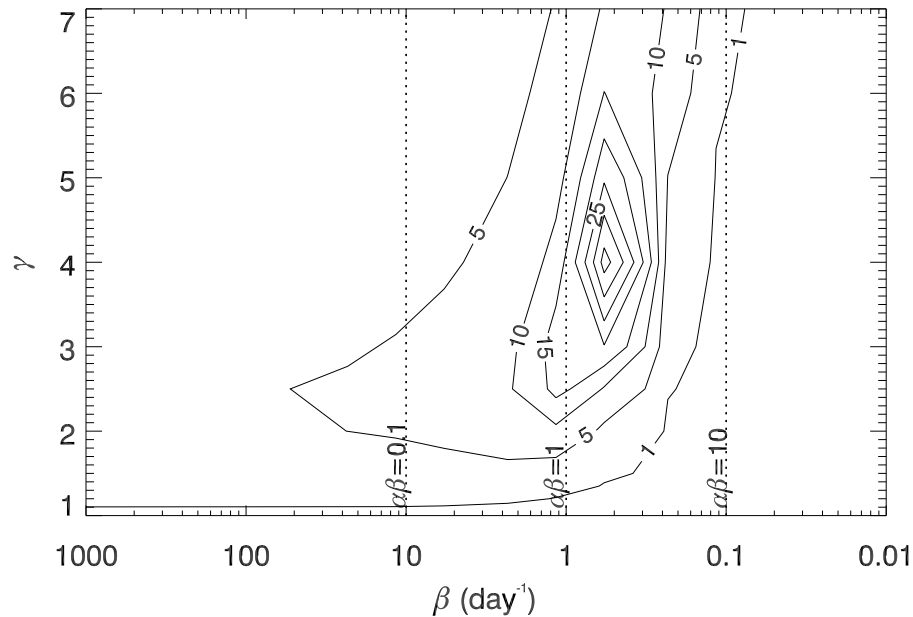


**Fig. 9.** Correlation between the diurnal cycles of percentage of tracer in the coastal outflow layer in the MetUM simulation and box-model divided by the root mean square difference between the diurnal cycles. Tracer has 24 h lifetime. The maximum indicates best parameter fit maximising correlation/bias.

Title Page

Abstract

Introduction

Conclusions

References

Tables

Figures

◀

▶

◀

▶

Back

Close

Full Screen / Esc

Printer-friendly Version

Interactive Discussion



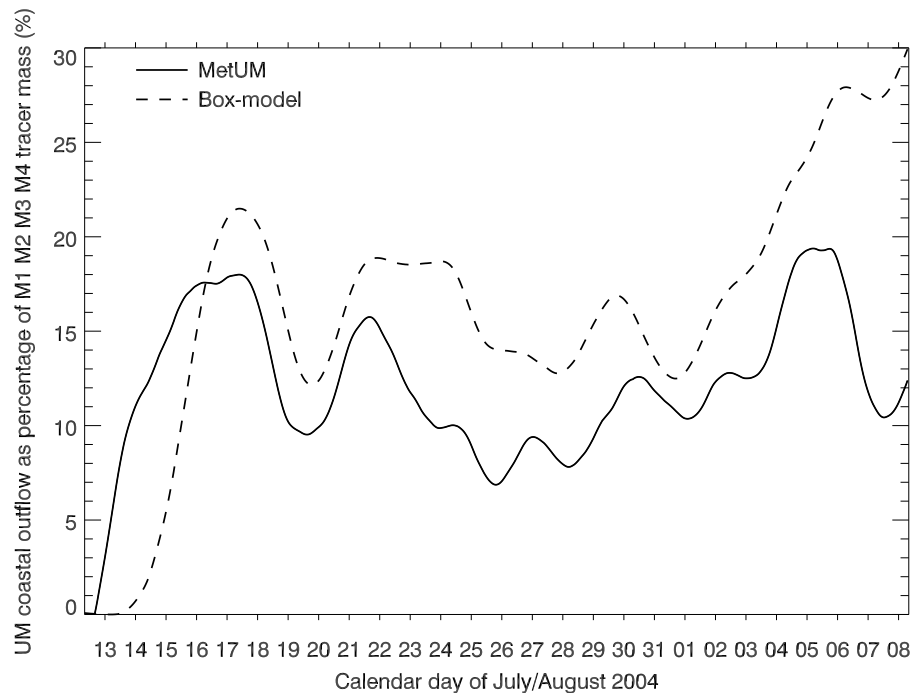


**Fig. 10.** Timeseries of tracer in the coastal outflow layer as a percentage of  $M_1 + M_2 + M_3 + M_4$ . Comparing the MetUM simulation (solid line) and box-model (dashed lines) forced with the cross-coastal wind speeds at 850 hPa obtained by averaging along the coast and filtering out the diurnal cycle.

Coastal outflow

D. L. Peake et al.

Title Page

Abstract Introduction

Conclusions References

Tables Figures

◀ ▶

◀ ▶

Back Close

Full Screen / Esc

Printer-friendly Version

Interactive Discussion

